

Dielectric Response of Deeply Supercooled Hydration Water in the Connective Tissue Proteins Collagen and Elastin

Catalin Gainaru,* Ariane Fillmer, and Roland Böhmer

Fakultät für Physik, Technische Universität Dortmund, 44221 Dortmund, Germany

Received: July 13, 2009; Revised Manuscript Received: August 14, 2009

The low-temperature dielectric relaxation of collagen and elastin was studied over a wide range of hydrations h . The hydration-shell response increases weakly with temperature, is thermally activated, and conforms to energy barrier scaling. This demonstrates the existence of a decoupled, secondary relaxation akin to that in binary structural glasses. Indications for fragile-to-strong transitions and other changes of mechanism are not found for hydrated collagen and elastin. For low h , the dielectric strength increases superlinearly with h ; concomitantly, the water molecules trigger significant mobility of the protein surface.

1. Introduction

Life on earth is based on liquid water with its fascinating complexities.¹ Its presence is essential for the dynamics and hence functionality of proteins. It has long been known that water covering protein surfaces does not crystallize down to low temperatures,² but the mechanisms governing the slowing down of hydration-shell water are currently a matter of stimulating debate. The dynamics of cold, hydrated proteins resembles that of glass formers, and assignments in terms of α - and β -relaxations have been made.³ These relaxations were variously linked to a transition of the protein, typically located near 225 K, or of the solvent at around 200 K. Also, a protein transition occurring as a consequence of a strong-to-fragile crossover of the hydration water was proposed.⁴ The existence of solvent⁵ and of protein transitions was recently questioned.⁶ Also, the nature of the dynamics prevailing at $T < 200$ K is disputed. While some researchers invoke a structural α -relaxation under conditions of spatial confinement,⁷ others argue in favor of decoupled β -relaxations,⁸ and also defect diffusion was proposed to be important.^{6,9}

Much of the recent low-temperature work focused on globular proteins such as myoglobin and hemoglobin, but the hydrated connective tissue proteins elastin (E) and collagen (C) are also attracting increasing interest.^{6,10} While E possesses a random coil conformation with a typical molecular weight of about 70 kDa or 800 amino acids, C is built from fibril-forming triple helices with ~ 1050 amino acids in each helix.¹¹ A calorimetric glass transition could be identified for hydrated E near physiological temperatures,¹² but C does not exhibit such a transition. In spite of these differences, our broadband dielectric measurements reveal that their hydration-shell behavior is virtually identical.

2. Samples

Lyophilized C from the bovine achilles tendon and E from the bovine neck ligament were obtained from Sigma Aldrich,

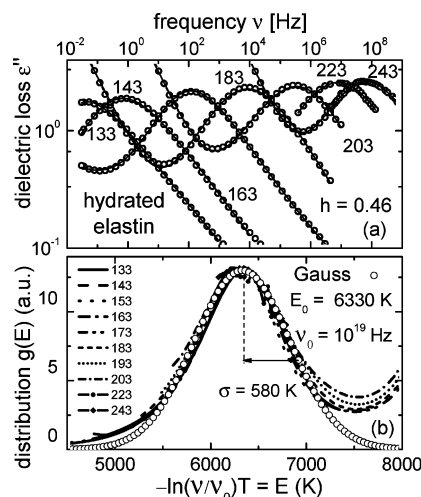


Figure 1. (a) Dielectric loss spectra of E46 recorded at various temperatures given in kelvin. (b) Frequency dependent losses, represented as lines, are scaled in a way so that a master curve emerges. This is achieved best for the given choice of ν_0 and then yields a maximum at $E = 6330$ K. For comparison, the circles represent a Gaussian distribution of energy barriers with a variance σ . The seeming deviation from that distribution at large energies is due to electrical conductivity.

dried, and checked for residual water using high-resolution proton NMR. Appropriate masses m of protein and bidistilled water were mixed to give the desired hydration level, $h = m_{\text{H}_2\text{O}}/m_{\text{C,E}}$. The samples are referred to as “E” or “C” followed by the effective h value in percent.

3. Results and Discussion

Dielectric loss spectra $\epsilon''(\omega)$ acquired for E46 in a broad frequency range are shown in Figure 1a. The peak frequencies ν_{max} follow an Arrhenius dependence, $\tau = (2\pi\nu_{\text{max}})^{-1} = \nu_0^{-1} \exp(E_a/T)$, over the entire T range; see Figure 2a. For ν_0 , we find $1 \times 10^{19} \text{ s}^{-1}$ and the resulting energy barrier is $E_a = 6330$ K or 0.55 eV. This value appears as universal for the

* To whom correspondence should be addressed. E-mail: catalin.gainaru@uni-dortmund.de. Phone: +49-231-7553517. Fax: +49-231-7553516.

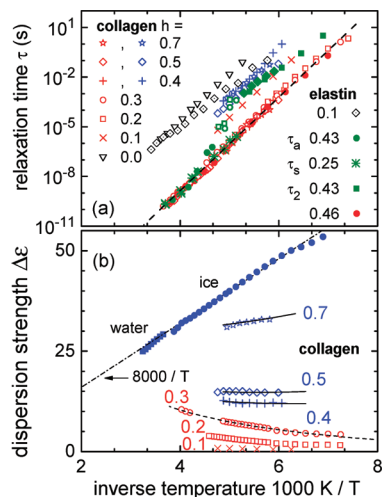


Figure 2. (a) Time constants characterizing E and C. The dielectric data are from this work except those for E10.¹⁰ The time constants from NMR (green symbols) were obtained in ref 6 using different techniques or different methods of analysis. They are represented by the same type of symbols as in ref 6. The dashed line corresponds to an activation energy of 6330 K. (b) Open symbols and crosses: Dispersion strengths resulting from HN fits described in the text. To present all $\Delta\epsilon$ data compactly, $\Delta\epsilon$ for liquid²⁵ and solid H₂O was divided by a factor of 3. The $\Delta\epsilon(T)$ dependences represented by the dashed and dashed-dotted lines were used to calculate the solid lines via eq 2. The red and blue symbols correspond to hydration water and involve (excess) ice, respectively.

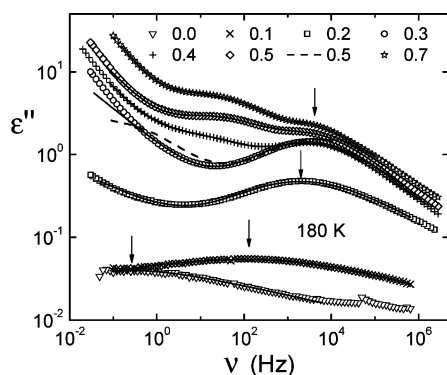


Figure 3. Isothermal dielectric loss of collagen for various h . The solid lines are HN fits to the data. The dashed line represents a measurement recorded subsequent to electrical cleaning. The arrows highlight the hydration-induced acceleration of the dipolar response for $h \leq h_c$.

hydration dynamics^{7,13} and corresponds to the energy required to break two H-bonds.

In order to appreciate the impact of hydration on the dipolar response, loss spectra at $T = 180$ K are shown in Figure 3 for C samples with $0 \leq h \leq 0.7$.¹⁴ Nominally dry C contains about 7% of structural water inside its triple helix and exhibits a very weak and relatively slow dielectric relaxation.¹⁵ Admixture of water leads to a peak at larger frequencies and with much increased strength $\Delta\epsilon$. For $h \geq 0.3$, the peak frequency ν_{\max} as well as $\Delta\epsilon$ saturate.

Thus, with growing h , the protein surface is increasingly covered with supercoolable water until a thin coating, probably a hydration monolayer, emerges at a critical level h_c . From our data, we find $h_c \approx 0.3$ for the C and ≈ 0.46 for the E system,¹⁴ in accordance with previous estimates.² The relaxation times obtained from the loss maxima of hydrated C and those of E46 are included in Figure 2a. They fully agree with each other. It is clear that these loss peaks are due to the motion in the

protein's hydration shell. Below, we address the question of whether the peaks solely reflect the motion of hydration water (HW) on a fixed protein surface or whether the activation of protein mobility is involved.

For $h > 0.3$, a low-frequency peak appears, gaining significant intensity with increasing h ; cf. Figure 3, which represents excess, crystallizable ice (EI). We analyzed our data using a Havriliak–Negami (HN) function $\epsilon'' = \text{Im}\{\sum_k \Delta\epsilon_k [1 + (2\pi\nu\tau_k)^{\alpha_k}]^{-\gamma_k}\} + A\nu^{-1}$. Here, k numbers relaxation processes with strengths $\Delta\epsilon_k$ and α_k as well as γ_k account for the several decades wide line shapes. A is a measure for the dc electrical conductivity. For $h \leq h_c$, a single relaxation process suffices to parametrize the data; cf. Figure 1a. For larger h , a weighted superposition of processes relating to HW and to EI is needed to describe the data; see the solid lines in Figure 3. The EI time constants depend only very slightly on h ; see Figure 2. For the HW, not only the relaxation times but the entire shapes of the loss peaks agree for $h > h_c$.

From free fits, a reliable determination of the shape parameters is difficult for $h > h_c$ because several loss peaks overlap and the conductivity contribution¹⁶ partially masks that of the EI. To remedy this problem, dc bias voltages ≥ 10 V were applied prior to measurements of C50 samples near 5 °C for several hours. As can be seen in Figure 3, this “electrical cleaning” procedure¹⁷ shifts the EI peak so that the low-frequency flank of the HW loss peak, in which we are most interested, is clearly visible. The relaxation times from and the shapes of the unmasked HW peaks coincide with those in C30. There are no signs of detrimental effects¹⁸ on the hydrated protein at the employed voltage levels. Thus, the behavior of the hydration layer is governed by the protein surface and practically unaffected by H₂O in more distant shells.

A line shape analysis of $\epsilon''(\nu)$ is also possible via appropriate scaling. If a distribution of energy barriers $G(E)$ is responsible for the observed symmetric broadening, a feature generally characterizing the β -relaxation in glasses,¹⁹ then the loss can be written as

$$\epsilon''(\nu) = \Delta\epsilon \int \frac{2\pi\nu\tau(E)G(E) dE}{1 + [2\pi\nu\tau(E)]^2} \quad (1)$$

In our case, the thermally activated loss peaks and hence $G(E)$ are so broad that one directly obtains $G(E) = G(T \ln \nu_0/\nu) \approx 2\epsilon''(\nu)/(\pi T \Delta\epsilon)$ from eq 1²⁰ if scaling works. It indeed does, as demonstrated in Figure 1b for E46. The shape of the resulting distribution can be approximated by a Gaussian, $G(E) \propto \exp[-(E - E_a)/(2\sigma^2)]$ with a standard deviation $\sigma \sim 580$ K, a value typical for β -processes in small-molecule glass formers.²¹

$\Delta\epsilon$ can be rationalized over the entire h range: For $h < h_c$, the relaxation strengths from the HN analysis and from scaling both reveal a tendency to increase slightly with T ; cf. Figure 2b. For C30, we find that $\Delta\epsilon_c = -3.58 + 0.0547[T/K]$ describes the data; cf. the dashed line in Figure 2b. Such a dependence resembles that of β -relaxations in organic glasses and also in some binary systems; see, e.g., refs 22 and 23. It is thus markedly different from the Curie-like behavior ($\Delta\epsilon \sim 1/T$) characterizing the susceptibility, e.g., of the α -relaxation in glass formers or of defect diffusion processes in ice.

A quantitative description of the $\Delta\epsilon$ data in the hydrated proteins can be achieved for $h > h_c$ as follows: The volume of EI can be determined via $h = (m_{\text{ice}} + m_c)/m_{\text{prot}} = \rho_{\text{ice}}V_{\text{ice}}(h)/m_{\text{prot}} + h_c$, where ρ_{ice} is then taken as the density of bulk ice. The volume fraction of EI is $y_{\text{ice}}(h) = V_{\text{ice}}(h)/V_{\text{tot}}$, with V_{tot}

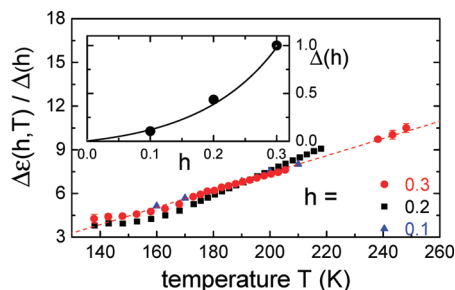


Figure 4. The scaled dispersion strength of collagen is practically independent of $h \leq h_c$. The scaling factor $\Delta(h)$ is depicted in the inset. The solid line emphasizes the superlinear increase of $\Delta\epsilon$ with h . The dashed line describes $\Delta\epsilon$ for $h = 0.3$ and is the same as that in Figure 2b.

denoting the total, fixed gap volume of the dielectric cell. Furthermore, the local layering of different dielectrics in overall isotropic environments leads to an effective dielectric constant¹⁵ which for the contribution of the EI to the dispersion step reads

$$\Delta\epsilon_{\text{eff,ice}} = \frac{2}{3}[\Delta\epsilon_c^{-1} + y_{\text{ice}}(\Delta\epsilon_{\text{ice}}^{-1} - \Delta\epsilon_c^{-1})] + \frac{1}{3}[\Delta\epsilon_c + y_{\text{ice}}(\Delta\epsilon_{\text{ice}} - \Delta\epsilon_c)] \quad (2)$$

Here, $\Delta\epsilon_{\text{ice}}$ varies as $\Delta\epsilon_{\text{ice}} = 24000/T[\text{K}]^{24}$ and parametrizes also the liquid-state data²⁵ well; cf. Figure 2b. The solid lines in Figure 2b are calculated for the EI component in the overhydrated samples using eq 2 and describe $\Delta\epsilon_{\text{EI}}$ from the HN analysis quantitatively, demonstrating that the relaxation in the hydration shell is unaffected by the presence of EI and vice versa. The behavior for $h > h_c$ is thus completely explained with reference to ice and to C30 with its fully developed hydration layer.

Let us now deal with the regime $h < h_c$. In Figure 4, using a factor $\Delta(h)$, we scaled $\Delta\epsilon$ for samples with $h \leq 0.3$ and find that $\Delta\epsilon$ always follows the same T dependence. However, $\Delta(h)$ increases much stronger than the number of water molecules in the hydration shell, indicating that a larger degree of hydration leads to an enhanced mobility of the protein surface itself. A sufficiently mobile protein surface promotes the isotropization of the motion of the water molecules. Furthermore, the dynamics at the protein surface speeds up if water is added to it, which seems to be a general phenomenon.²⁶ The corresponding changes in the relaxation rates are highlighted by the arrows in Figure 3 for C at $h \leq h_c$. The same trend emerges for the dielectric relaxation times of elastin: E10¹⁰ exhibits a dynamics that is much slower than that of elastin with $h = 0.46$, see Figure 2a, and higher h .¹⁴

In ref 6, a narrow, central line was found by deuteron NMR for hydrated collagen and elastin at $T > 200$ K. This observation does not rule out the existence of a secondary relaxation in the glass.²⁷ On the contrary, for the secondary relaxation of binary glass formers, sharp features in NMR spectra are well-known.²⁸ For some amorphous host–guest systems, these were tentatively assigned to arise from translational jump processes of the guest molecules.²⁹ In a hydrated protein, as another example of a binary glass former, the H₂O guests may also perform translational jumps even in the glassy state: After all, the activation energy that we find corresponds to that required to break two H-bonds.

In Figure 2a, the dielectric time constants are compared with correlation times from an NMR study on hydrated C and E.⁶

On the basis of the analysis of spin–lattice relaxation, the time scales τ_s or τ_a were deduced by assuming symmetric or asymmetric τ distributions, respectively. Furthermore, decay times τ_2 from stimulated-echo (STE) experiments⁶ are included in Figure 2a. The $\tau_s(T)$ data perfectly agree with our dielectric data,³⁰ indicating that a symmetric τ distribution is in fact also appropriate for the NMR data. STE experiments³¹ of bulk ice revealed that its dynamics is governed by defect diffusion involving tetrahedral jumps of water molecules. Distorted tetrahedral jumps were held responsible for the STE observations also in hydrated C and E.⁶ In this context, it is important to reiterate that the Curie-like dielectric strength accompanying defect diffusion in ice, cf. Figure 2b, is opposite to the $\Delta\epsilon(T)$ trend in hydrated proteins; see Figure 4. Furthermore, a change of reorientation mechanism³² is not indicated by the smooth temperature evolution of $\Delta\epsilon(T)$; see Figure 4.

4. Conclusions

An Arrhenius dependence is observed for hydration water in elastin and collagen over the entire temperature range. The dielectric contribution of their hydrated shells increases weakly with T , reveals scaling that implies a Gaussian distribution of energy barriers, and exhibits thermally activated dynamics. These features all testify to the existence of a β -relaxation and rule out defect diffusion from being important for the presently investigated proteins. The reorientation of water alone cannot explain the compositional evolution of the dielectric dispersion in underhydrated conditions: The approximate superlinear increase of $\Delta\epsilon(h)$ and the hydration-induced speed-up of the overall dynamics reveal that the motion of the protein surface itself plays an important role.

References and Notes

- (1) Angell, C. A. Insights into Phases of Liquid Water from Study of Its Unusual Glass-Forming Properties. *Science* **2008**, *319*, 582.
- (2) Dehl, R. E. Collagen: Mobile Water Content of Frozen Fibers. *Science* **1970**, *170*, 738.
- (3) Fenimore, P. W.; Frauenfelder, H.; McMahon, B. H.; Young, R. D. Bulk-solvent and hydration-shell fluctuations, similar to α - and β -fluctuations in glasses, control protein motions and functions. *Proc. Natl. Acad. Sci.* **2004**, *101*, 14408.
- (4) Lagi, M.; Chu, X.; Kim, C.; Mallamace, F.; Baglioni, P.; Chen, S.-H. The Low-Temperature Dynamic Crossover Phenomenon in Protein Hydration Water: Simulations vs Experiments. *J. Phys. Chem. B* **2008**, *112*, 1571.
- (5) Pawlus, S.; Khodadadi, S.; Sokolov, A. P. Conductivity in Hydrated Proteins: No Signs of the Fragile-to-Strong Crossover. *Phys. Rev. Lett.* **2008**, *100*, 108103. Khodadadi, S.; Pawlus, S.; Roh, J. H.; Garcia Sakai, V.; Mamontov, E.; Sokolov, A. P. The origin of the dynamic transition in proteins. *J. Chem. Phys.* **2008**, *128*, 195106.
- (6) Vogel, M. Origins of Apparent Fragile-to-Strong Transitions of Protein Hydration Waters. *Phys. Rev. Lett.* **2008**, *101*, 225701.
- (7) Cerveny, S.; Alegria, A.; Colmenero, J. Universal features of water dynamics in solutions of hydrophilic polymers, biopolymers, and small glass-forming materials. *Phys. Rev. E* **2008**, *77*, 031803.
- (8) Ngai, K. L.; Capaccioli, S.; Shinyashiki, N. The Protein “Glass” Transition and the Role of the Solvent. *J. Phys. Chem. B* **2008**, *112*, 3826.
- (9) Swenson, J.; Jansson, H.; Hedstroem, J.; Bergman, R. Properties of hydration water and its role in protein dynamics. *J. Phys.: Condens. Matter* **2007**, *19*, 205109.
- (10) Samouillan, V.; Andre, C.; Dandurand, J.; Lacabanne, C. Effect of Water on the Molecular Mobility of Elastin. *Biomacromolecules* **2004**, *5*, 958.
- (11) Banga, I. *Structure and Function of Elastin and Collagen*; Akadémiai Kiadó: Budapest, Hungary, 1966.
- (12) Kakivaya, S. R.; Hoeve, C. A. J. Glass point of elastin. *Proc. Natl. Acad. Sci.* **1975**, *72*, 3505, and ref 10.
- (13) Cerveny, S.; Schwartz, G. A.; Bergman, R.; Swenson, J. Glass Transition and Relaxation Processes in Supercooled Water. *Phys. Rev. Lett.* **2004**, *93*, 245702.
- (14) For elastin hydrated at other levels, see A. Fillmer et al. (to be published).

- (15) Fillmer, A.; Gainaru, C.; Böhmer, R. Broadened dielectric loss spectra and reduced dispersion strength of viscous glycerol in a connective tissue protein. *J. Non-Cryst. Solids*, in press.
- (16) Full dependences of fit parameters including conductivity can be found in ref 14.
- (17) Nazemi, A.; Williams, G.; Attard, G. S.; Karasz, F. E. The alignment of LC side-chain polymers in directing electric fields: theory and practice. *Polym. Adv. Technol.* **1992**, *3*, 157, and references cited therein. G. Williams is thanked for drawing our attention to this and related references.
- (18) Neumann, E. Chemical electric field effects in biological macromolecules. *Prog. Biophys. Mol. Biol.* **1986**, *47*, 197.
- (19) See, e.g.: Vogel, M.; Medick, P.; Rössler, E. Secondary Relaxation Processes in Molecular Glasses Studied by Nuclear Magnetic Resonance Spectroscopy. *Annu. Rep. NMR Spectrosc.* **2005**, *56*, 231.
- (20) Courtens, E. Scaling dielectric data on $\text{Rb}_{1-x}(\text{NH}_4)_x\text{H}_2\text{PO}_4$ structural glasses and their deuterated isomorphs. *Phys. Rev. B* **1986**, *33*, 2975. Brückner, H. J.; Courtens, E.; Unruh, H.-G. Dielectric relaxation of mixed crystals of $\text{Rb}_{1-x}(\text{NH}_4)_x\text{H}_2\text{PO}_4$ at microwave frequencies. *Z. Phys. B* **1988**, *73*, 337.
- (21) Kudlik, A.; Benkhof, S.; Blochowicz, T.; Tschirwitz, C.; Rössler, E. The dielectric response of simple organic glass formers. *J. Mol. Struct.* **1999**, *479*, 201.
- (22) Döb, A.; Paluch, M.; Sillescu, H.; Hinze, G. From Strong to Fragile Glass Formers: Secondary Relaxation in Polyalcohols. *Phys. Rev. Lett.* **2002**, *88*, 095701.
- (23) Capaccioli, S.; Ngai, K. L.; Shinyashiki, N. The Johari-Goldstein α -Relaxation of Water. *J. Phys. Chem. B* **2007**, *111*, 8197.
- (24) $\Delta\epsilon_{\text{ice}}$ is from the present work and agrees with, e.g.: Johari, G. P.; Jones, S. J. Dielectric Properties of Polycrystalline D_2O Ice Ih (hexagonal). *Proc. R. Soc. London, Ser. A* **1976**, *349*, 467.
- (25) Buchner, R.; Barthel, J.; Stauber, J. The dielectric relaxation of water between 0°C and 35°C. *Chem. Phys. Lett.* **1999**, *306*, 57.
- (26) Cervený, S.; Alegria, A.; Colmenero, J. Broadband dielectric investigation on poly(vinyl pyrrolidone) and its water mixtures. *J. Chem. Phys.* **2008**, *128*, 044901.
- (27) For example, for E46, the glass transition temperature is $T_g \approx 275$ K; see ref 10.
- (28) Böhmer, R.; Diezemann, G.; Hinze, G.; Rössler, E. Dynamics of supercooled liquids and glassy solids. *Prog. Nucl. Magn. Reson. Spectrosc.* **2001**, *39*, 191.
- (29) Medick, P.; Vogel, M.; Rössler, E. Large angle jumps of small molecules in amorphous matrices analyzed by 2D exchange NMR. *J. Magn. Reson.* **2002**, *159*, 126.
- (30) In ref 6, a T independent distribution width was assumed, different from what is implied by the scaling in Figure 1b. Agreement is nevertheless obtained, since the T_1 measurements cover a comparatively small T range.
- (31) Geil, B.; Kirschgen, T. M.; Fujara, F. Mechanism of proton transport in hexagonal ice. *Phys. Rev. B* **2005**, *72*, 014304.
- (32) Lusceac, S. A.; Herbers, C. R.; Vogel, M. ^2H and ^{13}C NMR studies on the temperature-dependent water and protein dynamics in hydrated elastin, myoglobin, and collagen. Cond-mat/0904.4424, 2009.

JP9065899